

## Design and Pharmacological Characterization of Inhibitors of Amantadine-Resistant Mutants of the M2 Ion Channel of Influenza A Virus<sup>†</sup>

Victoria Balannik,<sup>‡,§</sup> Jun Wang,<sup>‡,§</sup> Yuki Ohigashi,<sup>‡</sup> Xianghong Jing,<sup>§</sup> Emma Magavern,<sup>‡</sup> Robert A. Lamb,<sup>§,||</sup>  
William F. DeGrado,<sup>‡,@</sup> and Lawrence H. Pinto<sup>\*,‡</sup>

<sup>‡</sup>*Department of Neurobiology and Physiology, and* <sup>§</sup>*Department of Biochemistry, Molecular Biology and Cell Biology, and*  
<sup>||</sup>*Howard Hughes Medical Institute, and Northwestern University, Evanston, Illinois 60208-3500, <sup>‡</sup>Department of Chemistry, and*  
<sup>@</sup>*Department of Biochemistry and Biophysics, School of Medicine, University of Pennsylvania, Philadelphia, Pennsylvania 19104-6059. #These authors contributed equally to this work.*

*Received August 17, 2009; Revised Manuscript Received November 9, 2009*

**ABSTRACT:** The A/M2 proton channel of influenza A virus is a target for the anti-influenza drugs amantadine and rimantadine, whose effectiveness was diminished by the appearance of naturally occurring point mutants in the A/M2 channel pore, among which the most common are S31N, V27A, and L26F. We have synthesized and characterized the properties of a series of compounds, originally derived from the A/M2 inhibitor BL-1743. A lead compound emerging from these investigations, spiro[5.5]undecan-3-amine, is an effective inhibitor of wild-type A/M2 channels and L26F and V27A mutant ion channels *in vitro* and also inhibits replication of recombinant mutant viruses bearing these mutations in plaque reduction assays. Differences in the inhibition kinetics between BL-1743, known to bind inside the A/M2 channel pore, and amantadine were exploited to demonstrate competition between these compounds, consistent with the conclusion that amantadine binds inside the channel pore. Inhibition by all of these compounds was shown to be voltage-independent, suggesting that their charged groups are within the N-terminal half of the pore, prior to the selectivity filter that defines the region over which the transmembrane potential occurs. These findings not only help to define the location and mechanism of binding of M2 channel-blocking drugs but also demonstrate the feasibility of discovering new inhibitors that target this binding site in a number of amantadine-resistant mutants.

Influenza A virus is a continuing cause of mortality and morbidity on an annual basis (1) and thus presents an important target for pharmaceutical investigation. Two classes of anti-influenza agents are available for human use: adamantane derivatives amantadine and rimantadine which target the virus A/M2 ion channel and oseltamivir and zanamivir, which target the viral surface protein neuroaminidase (2). The use of amantadine and rimantadine is limited by the wide distribution of drug-resistant virus variants, including the recently isolated influenza A (H1N1) virus (3–5).

The A/M2 protein of the influenza A virus forms a pH-gated proton channel that is essential for virus replication (6). The mature channel consists of four identical subunits of 96 amino acids; each subunit is a type III integral membrane protein (N<sub>out</sub>, C<sub>in</sub>) (7). The highly conserved H<sub>37</sub>xxxW<sub>41</sub> motif located in the single transmembrane domain of the protein is responsible for its channel activity and proton selectivity (7, 8). The activity of wild-type (wt) A/M2 channels is known to be efficiently inhibited by amantadine, BL-1743, and its derivative azaspiro[5.5]undecane [spiro piperidine **20** (Table 1)] (Figure 1) (2, 9, 10). Naturally

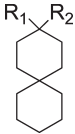
occurring point mutations of the pore-lining residues located outside of the H<sub>37</sub>xxxW<sub>41</sub> motif, such as L26F, V27A, A30T, S31N, and G34E, result in the formation of amantadine-insensitive influenza A virus phenotypes (3, 11–13). Extensive studies suggest that these residues are involved in the formation of the binding pocket for the drug (14–18). Amantadine-resistant phenotypes are prevalent in the currently circulating influenza A virus H3N2 and H1N1 2009 strains. Although the S31N mutation was observed in more than 90% of influenza A cases in certain years (19, 20), other amantadine-insensitive phenotypes like L26F and V27A were isolated from influenza A patients with emerging frequencies of 8–67% (19, 20). Other amantadine-resistant mutations have been found much less frequently (11, 20). Being resistant to amantadine, these naturally occurring mutants are also insensitive to all other known organic A/M2 channel inhibitors, including BL-1743 and spiro piperidine **20** (9, 10). Thus, there is a great need for novel anti-influenza drugs that target the most common amantadine-resistant phenotypes, S31N, V27A, and L26F (19, 20).

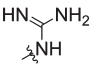
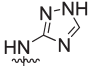
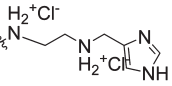
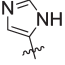
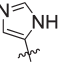
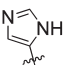
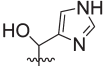
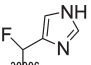
In this study, we synthesized a family of spiro[5.5]undecane compounds based on the structure of the previously investigated A/M2 channel inhibitor BL-1743. We found a simple amino derivative of BL-1743, spiro[5.5]undecan-3-amine [spiran amine **8** (Table 1)] to be effective not only for inhibition of the wt A/M2 channel but also for inhibition of two widely occurring amantadine-resistant mutants, L26F and V27A. The efficiency of this compound was investigated on A/M2 channels heterologously

<sup>†</sup>The research was supported by Grant GM56416 (W.F.D. and J.W.) and National Institutes of Health Research Grants R01 AI-57363 (L.H.P.), R01 AI-20201 (R.A.L.), and R01 AI-74517 (W.F.D. and J.W.). R. A.L. is an Investigator of the Howard Hughes Medical Institute.

\*To whom correspondence should be addressed: Department of Neurobiology and Physiology, Hogan Hall, 2205 Tech Dr., Northwestern University, Evanston, IL 60208-3500. Telephone: (847) 491-7915. Fax: (847) 491-5211. E-mail: larry-pinto@northwestern.edu.

Table 1: Inhibition Efficiency of the Synthesized Compounds on A/M2 Channels



Compound	R <sub>1</sub>	R <sub>2</sub>	AM2 channel activity after 100μM compound inhibition	IC <sub>50</sub> (μM)	K <sub>d</sub> (μM) <sup>a</sup>
Amantadine			6%	15.76±1.24	15.17
BL-1743			25%	45.31±3.92	193.54
8	H	NH <sub>3</sub> <sup>+</sup> Cl <sup>-</sup>	11%	12.59±1.11	9.16
9	H	NH <sub>2</sub> <sup>+</sup> Cl <sup>-</sup> CH <sub>3</sub>	8%	15.72±1.89	46.36
10	H		8%	14.60±1.70	11.50
11	H		25%	n.d	
12	H	NH <sub>2</sub> <sup>+</sup> Cl <sup>-</sup> (CH <sub>3</sub> ) <sub>2</sub> NH <sub>3</sub> <sup>+</sup> Cl <sup>-</sup>	100%	n.d	
13	H	NH <sub>2</sub> <sup>+</sup> Cl <sup>-</sup> (CH <sub>3</sub> ) <sub>3</sub> NH <sub>3</sub> <sup>+</sup> Cl <sup>-</sup>	100%	n.d	>500
14	H		91%	n.d	
15	OH		40%	n.d	
16	H		13%	12.54±1.24	
17	F		31%	57.57±2.24	
18	H		30%	n.d	
19	H		25%	29.19±1.46	
20			5%	0.92±0.11	12.87

<sup>a</sup>K<sub>d</sub> was obtained by global fitting of circular dichroism (CD) data of ligand titration to A/M2TM (22-46) using Igor Pro (wavemetrics). The variation of K<sub>d</sub> values is ±25% based on different fitting values obtained from three repeats of amantadine titration and two repeats of compound **20** titration. See the Supporting Information for details.

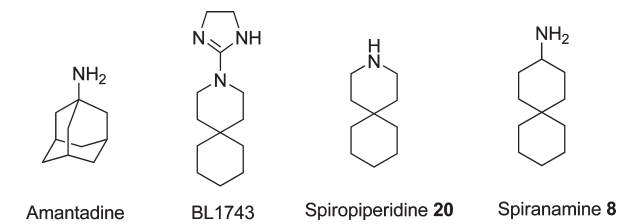


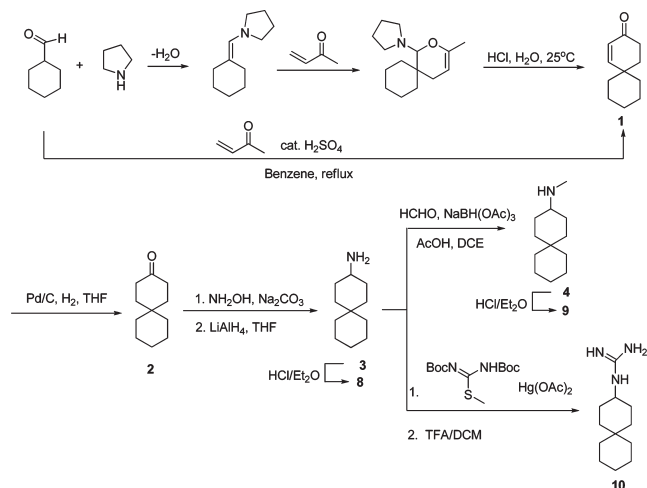
FIGURE 1: Chemical structures of A/M2 channel inhibitors.

expressed in *Xenopus* oocytes and confirmed by the *in vivo* plaque reduction assay of recombinant influenza A virus.

The pharmacologically relevant binding site for amantadine has been found to lie either inside (15) or outside (21, 22) the pore, although the physiological relevance of the latter finding has not been confirmed with either electrophysiology in oocytes or plaque reduction assays with recombinant virus (23). However, BL-1743

was shown to inhibit channel activity by binding inside the channel pore (24). Previous findings have shown that the kinetics of A/M2 channel inhibition by BL-1743 are more rapid than those reported for amantadine (9, 25), making it possible to test for competition between these drugs to determine whether they compete for the same binding site inside the channel pore. Our results support the previously published structural and functional studies that showed that amantadine inhibits the A/M2 channel by coordinating with pore-lining residues (12, 15, 16). We found that inhibition by amantadine, BL-1743, spiro piperidine **20**, and spiran amine **8**, all of which are positively charged at physiological pH, is independent of membrane voltage, consistent with binding in the N-terminal portion of the pore.

This study shows that a novel compound, spiran amine **8**, is a potent inhibitor of the L26F and V27A amantadine-resistant mutants of the A/M2 protein. Additional evidence supports the conclusion that amantadine binds inside the N-terminal half of

Scheme 1: Synthesis of Spiran Amine **8**, **9**, and Guanidine **10**

the channel pore. These findings show that novel anti-influenza drugs, capable of targeting wt and amantadine-resistant virus phenotypes, can be identified and that the N-terminal part of the pore is a good target for such drugs.

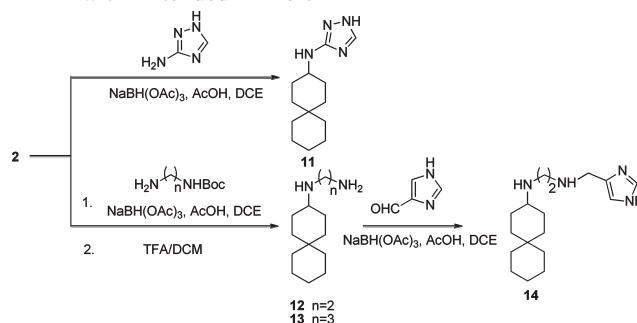
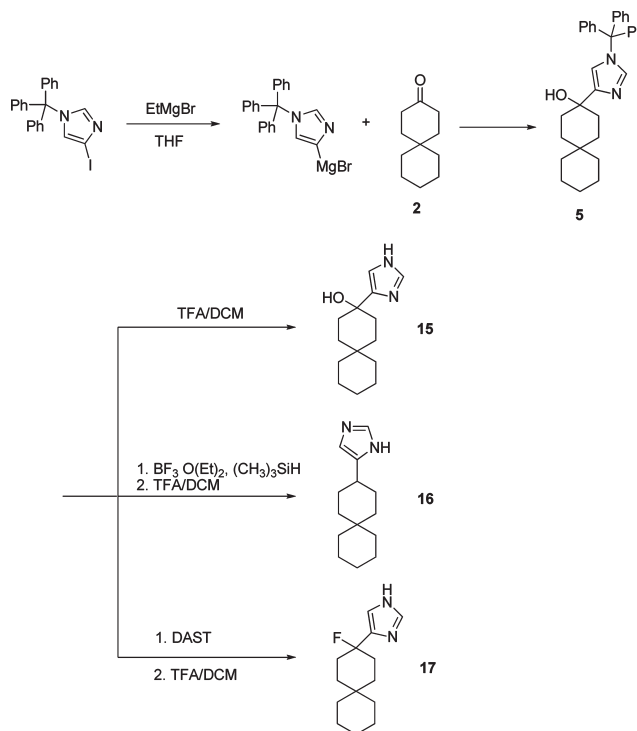
## MATERIALS AND METHODS

**Spiran A/M2 Inhibitor Library Synthesis.** The syntheses of the primary amine analogue (**8**) of spiropiperidine-azaspiro[5.5]undecane and the methyl-substituted secondary amine **9** are shown in Scheme 1. Intermediate spiro[5.5]undec-1-en-3-one **1** was prepared both from acid-catalyzed one-pot Robinson annulation reaction and through a Diels–Alder adduct followed by acid hydrolysis and aldol ring formation. The acid-catalyzed annulation often led to low yields ( $\leq 62\%$ ) due to acid-catalyzed polymerization of methyl vinyl ketone as evidenced by a black oily substance formed in the reaction flask (26). While catalysis with proline derivatives might allow circumvention of these problems, we found the alternative Diels–Alder route provided better overall yields (75%) (27). Hydrogenation of enone **1** with Pd/C with an  $H_2$  balloon gave spiro[5.5]undecan-3-one **2**. Conversion of ketone **2** to amine **8** was achieved by treatment with hydroxylamine followed by  $LiAlH_4$  reduction. Methylamine **9** was prepared by reductive amination of **8** with formaldehyde as reported.

Syntheses of spiran triazole **11** and spiran amines **12–14** with extended linkers in Scheme 2 were accomplished by reductive amination as described previously.

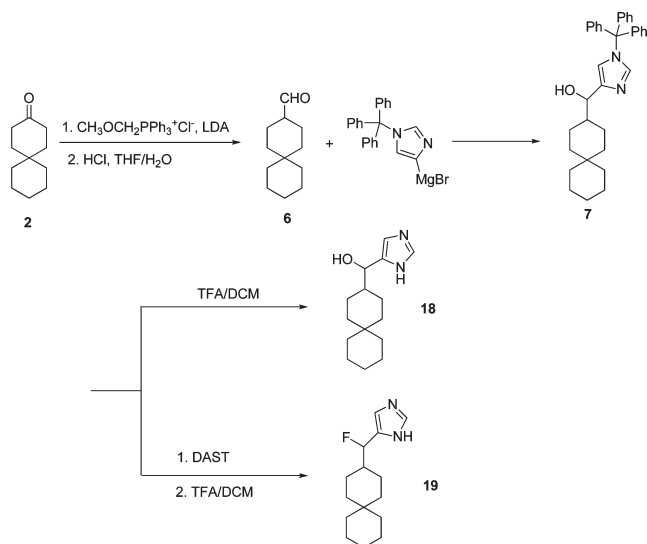
Compound **15**, with an imidazole headgroup, was synthesized by nucleophilic attack of imidazol-4-yl anion (generated by treatment of *N*-trityl 4-iodoimidazole) onto ketone **2** (28), followed by deprotection in a TFA/DCM mixture as shown in Scheme 3. The hydroxyl group in **15** was either reduced by  $Et_3SiH/BF_3 \cdot OEt_2$  to give **16** or fluorinated by DAST to give **17** after deprotection. Ketone **2** was converted to aldehyde **6** by the Wittig reaction, followed by acid hydrolysis. Compounds **18** and **19** were then synthesized from compound **6** in the same manner that was described for **15** and **17** (Scheme 4).

**Molecular Biology and in Vitro cRNA Transcription.** The cDNA encoding the influenza virus A/Udorn/72 A/M2 protein and the A/M2 amantadine-insensitive mutants were inserted into pGEMHJ (a gift from N. Dascal, Tel-Aviv University, Tel-Aviv, Israel) for the expression on *Xenopus* oocytes. cRNA was prepared as previously described (29).

Scheme 2: Synthesis of Spiran Triazole **11** and Spiran Amines **12–14** with Extended LinkersScheme 3: Synthesis of Spiran with an Imidazole Headgroup (**15–17**)

**Heterologous Expression and Electrophysiological Recordings.** Stage V–VI *Xenopus laevis* oocytes were prepared as described previously (30). Oocyte injection and TEVC electrophysiological measurements were conducted as previously described (29). Amantadine (Sigma, St. Louis, MO) was applied to inhibit A/M2-induced currents. Data were analyzed using ORIGIN version 8.0 (OriginLab, Northampton, MA).

**Cells, Viruses, and Plasmids.** 293T and Madin-Darby canine kidney (MDCK) cells were maintained in Dulbecco's modified Eagle's medium (DMEM) (Invitrogen, Carlsbad, CA) supplemented with 10% FBS. Influenza A/Udorn/72 virus (wt) and mutant viruses were propagated in MDCK cells overlaid with serum-free DMEM containing 3.0  $\mu\text{g/mL}$  *N*-acetyltrypsin (NAT) (Sigma-Aldrich, St. Louis, MO) at 37 °C. wt virus and mutant virus (V27A/L38F) were generated by using reverse genetics from cDNAs essentially as described previously (31). The eight genome-sense (pHH21) plasmids and four protein-expressing (pcDNA3.1) plasmids used to generate influenza virus by reverse genetics have been described previously (31). Mutation into the M2 gene in the pHH21 vector was generated using Quick Change mutagenesis (Stratagene, La Jolla, CA). 293T

Scheme 4: Synthesis of Spirans **18** and **19**

cells were transfected using TransIT-LT1 (Mirus, Madison, WI) according to the manufacturer's protocols. Virus stocks were propagated in MDCK cells, and the virus titers were determined by a plaque assay on MDCK cells. For determination of viral genome sequences, viral RNA was extracted by using the QIAamp viral RNA kit (Qiagen, Valencia, CA), followed by Super Reverse Transcriptase (Molecular Genetic Resources, Tampa, FL) and using genome-specific primers, and amplified with AmpliTaq DNA polymerase (Applied Biosystems, Foster City, CA). The complete nucleotide sequences of the M genes were determined using a 3100-Avant genetic analyzer (Applied Biosystems).

**Plaque Reduction Assays.** Confluent monolayers of MDCK cells were incubated with the wt Udorn virus [100 plaque-forming units (pfu) per well] and V27A/L38F mutant virus (1000 and 100 pfu per well) in a DMEM/1% bovine serum albumin mixture for 1 h at 37 °C. The inoculums were removed, and the cells were washed with phosphate-buffered saline (PBS). The cells were then overlaid with DMEM-containing 0.6% Avicel microcrystalline cellulose (FMC BioPolymer, Philadelphia, PA) and NAT (2.0  $\mu\text{g/mL}$ ). To examine the effect of drugs (BL-1743, spiran amines, and amantadine) on plaque formation, monolayers were preincubated with DMEM supplemented with the indicated concentrations of the drugs at 37 °C for 30 min, and virus samples were preincubated with a DMEM/1% BSA mixture with the indicated concentrations of the drugs at 4 °C for 30 min before infection. Two to three days after infection, the monolayers were fixed and stained with a naphthalene black dye solution (0.1% naphthalene black, 6% glacial acetic acid, and 1.36% anhydrous sodium acetate).

## RESULTS

**Structure–Activity Relationship (SAR) of 3-Substituted Spiro[5.5]undecanes.** Our previous SAR study of 2-[3-azaspiro(5.5)undecan-2-yl]-2-imidazoline (BL-1743) revealed a very potent spiro piperidine compound **20** with an  $\text{IC}_{50}$  of 0.9  $\mu\text{M}$  (10). However, compounds in this series failed to inhibit amantadine-resistant variants of A/M2, which prompted us to test alternative structures. In particular, a consideration of the overlay of the parent compound on derivatives of amantadine suggested that conversion of the piperidine in spiro piperidine **20** to a 3-aminocyclohexyl amine while maintaining the second spiro

six-membered ring would produce a more effective inhibitor. We therefore synthesized a family of spiro[5.5]undecanes, in which the 3-position was substituted with amines or other basic substituents (Table 1).

The compounds were tested on A/M2 channels expressed in *Xenopus* oocytes using the TEVC technique. The inhibitory effect of the compounds was confirmed by *in vivo* plaque reduction assays of influenza A virus (A/Udorn/72). The simple amino derivative, **8**, exhibited an activity on par with that of amantadine. However, further substitutions of the amine tended to cause a loss of activity. N-Methylation (compound **9**) led to a slightly less potent compound, while the guanidine derivative, **10**, had a potency similar to that of methylamine **9**. Modifying the amine by addition of polar substituents and extended linkers (compounds **11–14**) led to a marked decrease in activity. On the other hand, replacing the amine with an imidazole group caused a slight decrease in activity (compound **16**). We also examined additional substitutions at the 3-methylene of **16**, through the introduction of a hydroxyl and fluoro substituent in **15** and **17**, respectively. These substitutions gave rise to compounds with lower potency. Furthermore, the similarly substituted compounds **18** and **19** had decreased activity compared to that of primary amine **8**.

In summary, these data show that the primary amino group is likely to be a nearly optimal substituent for the spiro[5.5]undecane scaffold. We therefore turned our attention to determining how the piperidine for cyclohexylamine substitution in **20** versus **8** affected the ability of these compounds to inhibit amantadine-resistant forms of A/M2.

**Inhibition Effect of Spiran Amine Compound **8** on wt and Amantadine-Insensitive A/M2 Channels.** Amantadine-resistant mutants carry naturally occurring point mutations of the pore-lining residues of the A/M2 channel (3, 11, 12). Extensive structural, electrophysiological, and *in silico* investigations suggest that these residues form the binding pocket for the drug (14–18). We have tested the effect of spiran amine **8** on wt A/M2 channels and A/M2 channels with altered amantadine sensitivity and compared the inhibition by compound **8** to that of amantadine and BL-1743. We found that spiran amine **8** efficiently inhibits the activity of wt A/M2 channels and of A/M2-V27A mutants, with  $\text{IC}_{50}$  values of 12.6 and 84.9  $\mu\text{M}$ , respectively (Figure 2 and Table 2). The inhibition of V27A mutants is particularly interesting, given that amantadine, BL-1743, and spiro piperidine **20** gave less than 10% inhibition of the mutant, when applied at a concentration of 100  $\mu\text{M}$ . It is also interesting to note that the V27G mutant, which is also naturally occurring (32), is highly resistant to all compounds tested (Table 2).

We next examined the ability of compound **8** to inhibit other pore-lining mutants. S31N is a highly frequent mutation, which gives rise to a decreased sensitivity to amantadine [ $\text{IC}_{50}$  = 237.0  $\mu\text{M}$  vs 15.8  $\mu\text{M}$  for the wt A/M2 channel (Figure 2)], and complete resistance to rimantadine ( $\text{IC}_{50}$  > 10 mM). Similarly, compound **8** exhibited little inhibition of this mutant. Other mutations deeper inside the pore than V27 (A30T and G34E) completely eliminate the ability of all drugs tested to inhibit the channel (Table 2).

By contrast to the other mutations considered here, L26F does not involve a pore-lining residue and instead involves a partially largely lipid-exposed residue that packs at the interface between the helices adjacent to V27. Thus, this residue is expected to play a more subtle and less direct role in defining the steric properties of the drug-binding site. Indeed, amantadine inhibits this mutant



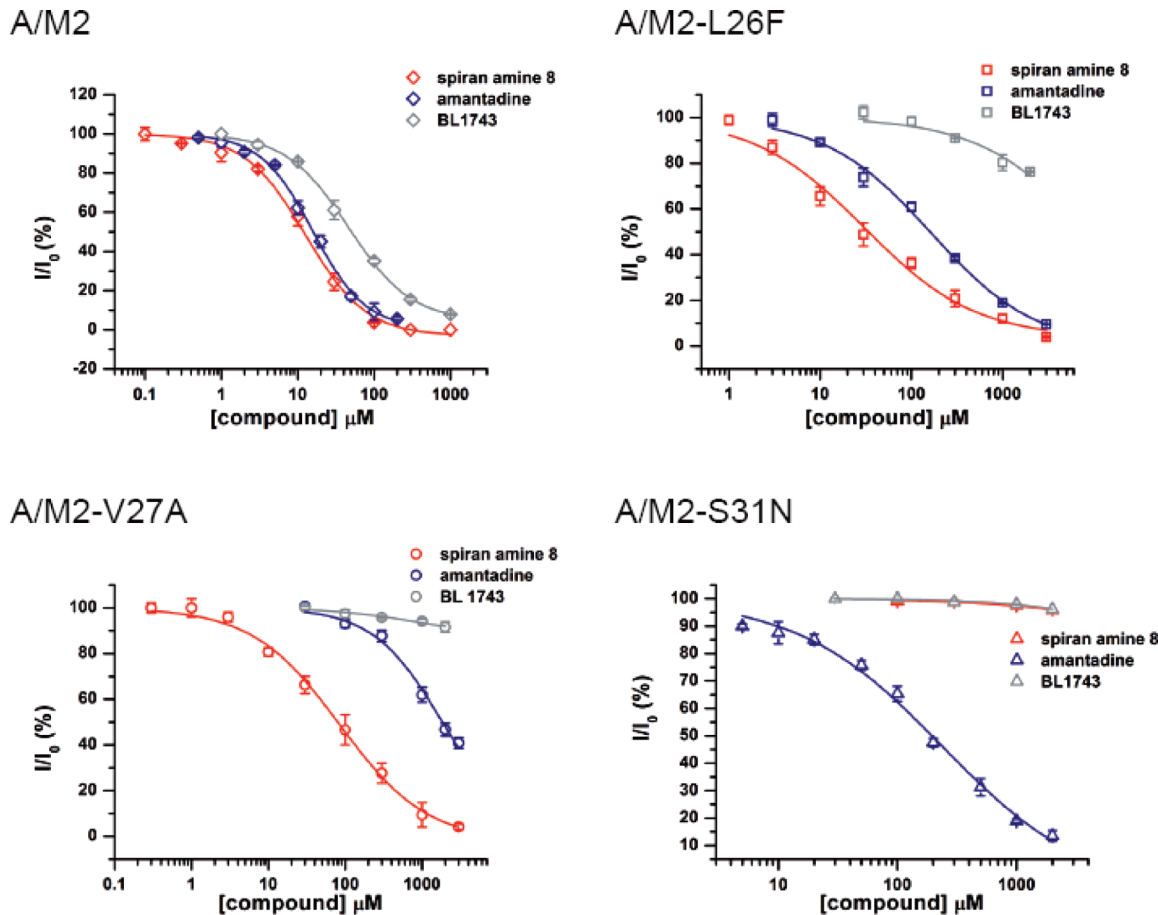


FIGURE 2: Inhibition efficiency of amantadine, BL-1743, and spiran amine **8** on wt A/M2 channels and A/M2 L26F, V27A, and S31N mutants. Channel activity was assayed by TEVC for A/M2 channels expressed in *Xenopus* oocytes. Responses in the presence of various concentrations of an inhibitor (I) were normalized to the current evoked by application of the activating (pH 5.5) solution without inhibitor ( $I_0$ ). The experimental data are the average of three independent experiments. Each point is the mean ( $\pm$ standard deviation) of five to eight oocytes. A/M2 with amantadine  $IC_{50} = 15.76 \pm 1.24 \mu M$ . A/M2 with BL-1743  $IC_{50} = 46.25 \pm 3.56 \mu M$ . A/M2 with spiran amine **8**  $IC_{50} = 12.59 \pm 1.11 \mu M$ . A/M2-L26F with amantadine  $IC_{50} = 164.46 \pm 14.40 \mu M$ ; A/M2-L26F with BL-1743  $IC_{50} > 10$  mM. A/M2-L26F with spiran amine **8**  $IC_{50} = 30.62 \pm 8.13 \mu M$ . A/M2-V27A with amantadine  $IC_{50} = 1840 \mu M$ . A/M2-V27A with BL-1743  $IC_{50} > 10$  mM. A/M2-V27A with spiran amine **8**  $IC_{50} = 84.92 \pm 13.61 \mu M$ . A/M2-S31N with amantadine  $IC_{50} = 237.01 \pm 22.14 \mu M$ . A/M2-S31N with BL-1743  $IC_{50} > 10$  mM. A/M2-S31N with spiran amine **8**  $IC_{50} > 10$  mM.

Table 2: Inhibition Effect of Amantadine, BL-1743, Spiran Amine **8**, and Spiran Amine **9** on wt A/M2 and Amantadine-Insensitive Mutant Channels<sup>a</sup>

	% remaining activity after application of 100 $\mu M$ compound			
	BL-1743	spiran amine <b>8</b>	spiran amine <b>9</b>	amantadine
A/M2-L26F	89.2 $\pm$ 4.8	32.4 $\pm$ 3.3	72.6 $\pm$ 8.4	51.8 $\pm$ 3.5
A/M2-V27A	97.4 $\pm$ 1.8	46.6 $\pm$ 6.6	70.2 $\pm$ 1.6	93.1 $\pm$ 1.9
A/M2-V27G	82.9 $\pm$ 9.3	87.9 $\pm$ 6.1	89.6 $\pm$ 4.1	95.0 $\pm$ 4.9
A/M2-A30T	102.0 $\pm$ 2.3	98.1 $\pm$ 7.0	101.2 $\pm$ 3.2	104.6 $\pm$ 4.3
A/M2-S31N	100.1 $\pm$ 0.7	99.1 $\pm$ 0.9	100.4 $\pm$ 4.1	65.3 $\pm$ 2.7
A/M2-G34E	89.8 $\pm$ 6.9	96.6 $\pm$ 5.9	101.7 $\pm$ 2.8	100.4 $\pm$ 6.7

<sup>a</sup>Data presented as a percent of remaining A/M2 activity after application of an inhibitor (100  $\mu M$ ) for 2 min. The experimental data are the average of three independent experiments. Each point is a mean ( $\pm$ standard deviation) of five to seven oocytes.

with reduced affinity ( $IC_{50} = 164.5 \mu M$ ), versus the much larger decreases seen for other variants. Compound **8** is an even more potent inhibitor of A/M2-L26F [ $IC_{50} = 30.6 \mu M$  (Figure 2)].

The inhibitory effect of compounds **8** and **9** on the recombinantly expressed A/M2 wt and mutant channels was confirmed

by *in vivo* plaque reduction assays of influenza A viruses. Plaque formation of wt influenza virus (A/Udorn/72) was inhibited by amantadine, **8**, and **9** at concentrations ranging from 0.5 to 5  $\mu M$  (Figure 3A), with compound **8** showing slightly more potent activity than compound **9**. BL-1743 inhibited wt virus plaque formation only at high concentrations (50–100  $\mu M$ ) (Figure 3B). On the other hand, the plaque count and size resulting from infection by influenza virus A/M2-V27A/L38F, which contains the M2-V27A mutation, were reduced by 50  $\mu M$  spiran amine **8** (Figure 3C). These findings are consistent with the electrophysiological data (Figure 1). In comparison, amantadine and BL-1743 in the same concentration range failed to inhibit plaque formation of A/M2-V27A/L38F viruses (Figure 3C). The L38F mutation is naturally found in the Weybridge strain of the virus. This mutation is pharmacologically silent to the drugs used and does not affect M2 channel function in electrophysiological recordings (25, 33, 34). The activity of the A/M2-V27A/L38F double mutant was tested by TEVC and compared to that of a A/M2-V27A single mutant. We found that the sensitivity of the double mutant channel to the tested compound was comparable to that of the A/M2-V27A single mutant. The A/M2-V27A/L38F mutant channels were not sensitive to either amantadine or BL-1743, while being efficiently inhibited by compound **8**

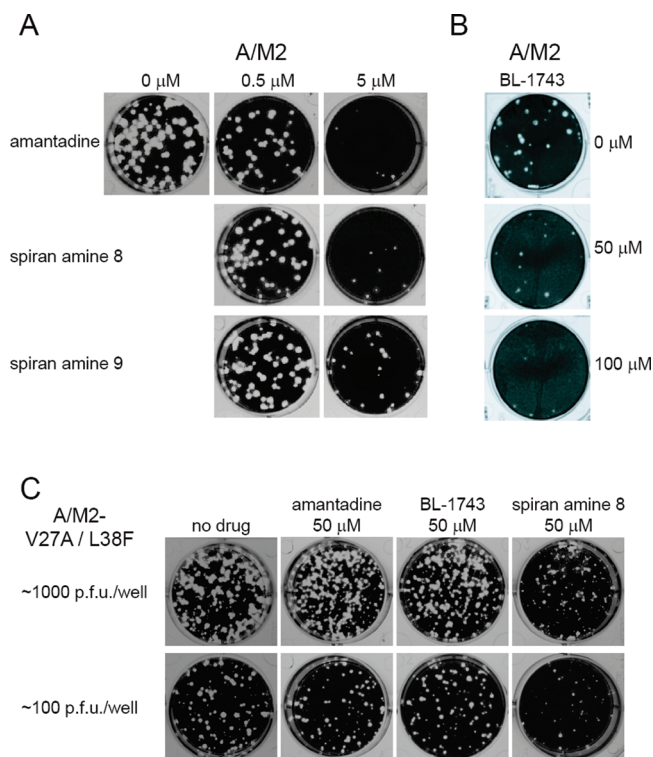


FIGURE 3: *In vivo* plaque reduction assay. wt influenza virus (A/Udorn/72) and influenza virus containing mutations in the M2 TM domain (V27A/L38F) were recovered from cloned DNA and assayed for plaque formation on MDCK cells in the presence or absence of drugs as described in Materials and Methods. (A) Effects of amantadine, BL-1743, and compounds **8** and **9** (0.5 and 5  $\mu$ M, respectively) on Udon plaque formation. (B) Effect of BL-1743 (50 and 100  $\mu$ M) on influenza virus plaque formation. (C) Effects of amantadine, BL-1743, and spiran amine **8** (50  $\mu$ M) on influenza mutant virus V27A/L38F plaque formation: (top panel)  $\sim$ 1000 pfu of mutant virus used per well and (bottom panel)  $\sim$ 100 pfu of mutant virus used per well. Plaque count: no drug, 99 plaques/well; 50  $\mu$ M amantadine, 82 plaques/well; 50  $\mu$ M BL-1743, 86 plaques/well; 50  $\mu$ M spiran amine **8**, 37 plaques/well.

(A/M2-V27A/L38F  $IC_{50}$  =  $78.21 \pm 15.06 \mu$ M; A/M2-V27A  $IC_{50}$  =  $84.92 \pm 13.61 \mu$ M). On the basis of these findings, we decided that the results of the plaque formation assay performed on the A/M2-V27A/L38F double mutant adequately represent the behavior of the A/M2-V27A single mutant.

Thus, spiran amine **8** is capable of efficiently inhibiting wt A/M2 channels and A/M2-L26F and A/M2-V27A mutant channels expressed in oocytes, and it also prevents replication of wt virus and these mutant recombinant viruses. As discussed below, we attribute the greater potency of compound **8** in the plaque assay versus the electrophysiological studies to kinetic effects arising from the slow kinetics of binding of this class of inhibitors. Compounds are incubated with oocytes for brief periods in the electrophysiological experiments, but for much longer periods in the plaque binding studies.

We also assessed the binding of selected drugs to the transmembrane domain of wt A/M2 protein (M2TM, residues 22–46), using a spectroscopic assay that relies upon changes in the CD spectrum of M2 induced by binding of drugs (Table 1 and described in the Supporting Information). All drugs bound with a stoichiometry of approximately one drug per tetramer. At pH 7.4, potent compounds were found to bind to the transmembrane tetrameric form of M2TM with low micromolar binding constants. Compounds **8** and **10** were found to be approximately

equipotent with amantadine, displaying dissociation constants in the range of 7–8  $\mu$ M (Table 1). In agreement with the plaque assay, compound **9** was approximately 4-fold less potent than amantadine or compound **8**. These data support the expectation that the drugs inhibit the channel activity by binding directly to the A/M2 proton channel.

**Competition among Inhibitors.** In 1999, Gandhi and co-workers concluded from competition experiments with Cu(II) that BL-1743 inhibits A/M2 channel activity by binding inside the channel pore (24). However, conflicting structural studies have shown that adamantane derivatives bind either inside (15) or outside (21) the channel pore, although the pharmacological relevance of the latter finding has not been confirmed (23). Furthermore, solid-state NMR experiments have shown that a member of the spiran series of compounds binds A/M2 in a manner similar to that of amantadine (10). Given that BL-1743 appears to bind within the pore, we were interested in determining whether amantadine binds competitively with respect to this compound or whether it binds to an independent site.

The second-order rate constant ( $\kappa_{on}$ ) for the association and inhibition of the wt A/M2 channel with BL-1743 was calculated to be  $720 \text{ M}^{-1} \text{ s}^{-1}$  (9), which is comparable with the  $\kappa_{on}$  of amantadine ( $600\text{--}900 \text{ M}^{-1} \text{ s}^{-1}$ ) (25). However, the dissociation rate constant ( $\kappa_{off}$ ) for BL-1743 is approximately 1 order of magnitude faster than that calculated for amantadine ( $10^{-3}$  and  $10^{-4} \text{ s}^{-1}$ , respectively) (9, 25). We exploited this difference in the  $\kappa_{off}$  values of BL-1743 and amantadine to investigate the mechanism of A/M2 channel inhibition by amantadine by testing whether this drug competes with BL-1743 for the inhibition of A/M2 channel activity. For these experiments, A/M2 channels were expressed in *Xenopus* oocytes, and the channel activity was assayed by TEVC. The A/M2 channel activity was evoked by application of the low-pH activating solution (pH 5.5). In the control experiments, the channel activity was inhibited by saturating concentrations of either BL-1743 (1000  $\mu$ M) or amantadine (100  $\mu$ M) alone (Figure 4A,B). As seen from panels A and B of Figure 4, the inhibition of A/M2 was essentially fully reversible in the time frame of 5 min for BL-1743, but only  $\sim$ 10% complete for amantadine. This finding is consistent with the slower off rate for amantadine than for BL-1743. Compound **8** also showed an off rate similar to that of amantadine, as expected from their similar  $IC_{50}$  values (Figures 2 and 4C).

We next examined the competition between BL-1743 and amantadine, chosen as a representative example of the slow dissociating class of inhibitors. We subjected the oocytes to sequential treatment with drugs and drug-free recording solutions in a manner designed to probe both the kinetic and thermodynamic aspects of inhibition. A resting oocyte, incubated in the nonactivating solution (pH 8.5), was treated as follows. (1) The oocyte was acidified by the application of the activating solution (pH 5.5) (red bar in Figure 5). (2) The oocyte was pulsed with the activation solution containing rapidly reversible BL-1743 at various concentrations ranging from 3 to 1000  $\mu$ M for 60 s (green bar). (3) BL-1743 in the activating solution was replaced with the slowly reversible inhibitor amantadine (100  $\mu$ M) for an additional 90 s (yellow bar). (4) The pH was shifted to 8.5 to allow the system to re-equilibrate for 5 min (second blue bar). (5) The oocyte was re-acidified (second red bar) and the degree of recovered channel activity was determined.

As expected from a reversible second-order binding event, the rate and extent of inhibition observed during the BL-1743

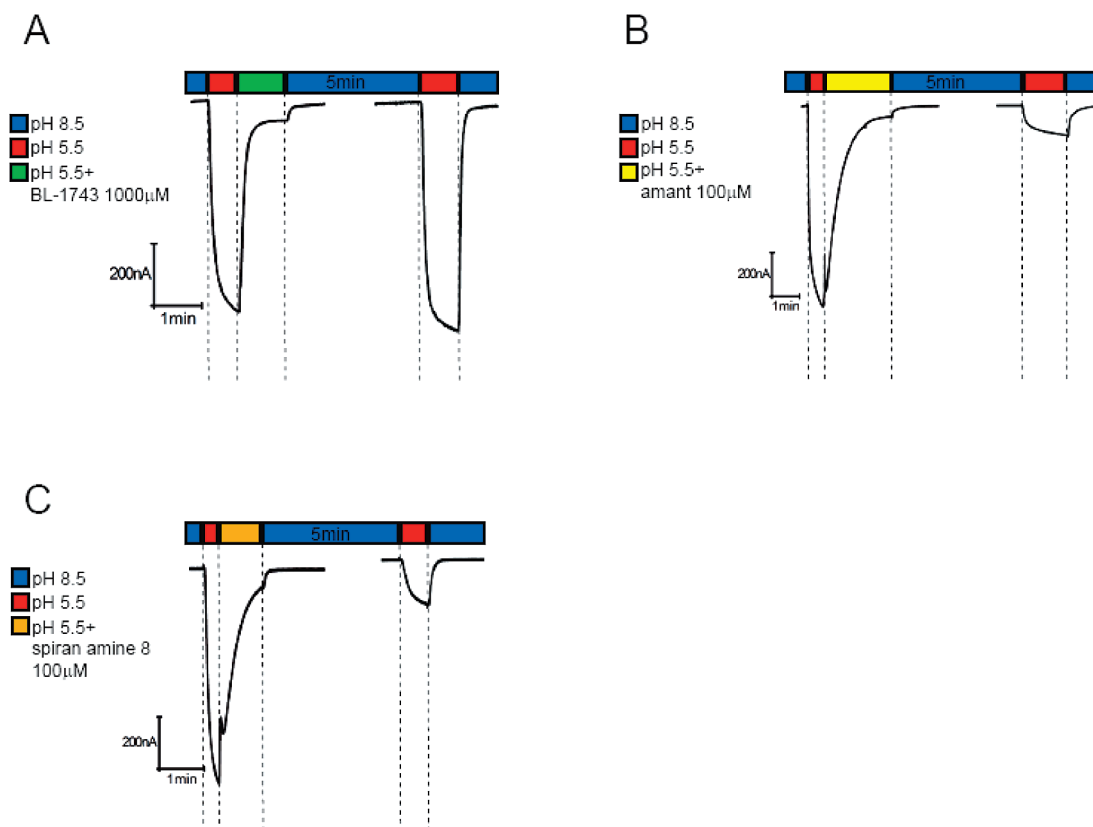


FIGURE 4: Inhibition of A/M2 channel activity by saturating concentrations of BL-1743, amantadine, and spiran amine **8**. (A–C) Representative traces of A/M2 channel activity inhibited by either BL-1743 [ $1000\ \mu\text{M}$  (A)], amantadine [ $100\ \mu\text{M}$  (B)], or spiran amine **8** [ $100\ \mu\text{M}$  (C)]. A/M2 channel activity was induced by application of the activating solution (pH 5.5, red horizontal bar above the trace). The currents were inhibited by the application of the activating solution containing either BL-1743 [green horizontal bar (A)], amantadine [yellow horizontal bar (B)], or spiran amine **8** [orange horizontal bar (C)] for 60–90 s. After the maximal inhibition was achieved, oocytes were superfused with the nonactivating solution (pH 8.5, second blue horizontal bar) for 5 min to allow current recovery and the channel activity was assayed again by the application of the activating solution (second red horizontal bar). Note that recovery was complete only for BL-1743.

incubation period increased in a concentration-dependent manner (Figure 5). The ensuing traces observed during the amantadine-chase period reflect several processes, including (a) the binding of amantadine to the fraction of channels that were not inhibited in the initial BL-1743 pulse, (b) dissociation of BL-1743 to generate uninhibited channels, and (c) binding of amantadine to newly uninhibited A/M2 channels following dissociation of BL-1743. With low concentrations of BL-1743, little inhibition was achieved; thus, upon addition of  $100\ \mu\text{M}$  amantadine, the kinetics were dominated by this process, and the trace approached a simple exponential decay (Figure 5A,B). On the other hand, with a  $1000\ \mu\text{M}$  BL-1743 pulse, inhibition was complete and the resulting traces reflected a competition between dissociation of BL-1743 and the on rate for amantadine binding, both of which occur with relaxation times on the second to minute time scale under these conditions (Figure 5D). Thus, biphasic kinetics were observed, with the rising phase reflecting the fact that as the BL-1743 dissociates from the channel, amantadine does not bind instantly, leading to a partial recovery followed by inhibition by amantadine at longer times. As expected, intermediate behavior was observed with an initial pulse of  $100\ \mu\text{M}$  BL-1743 (Figure 5C).

In the complementary experiments A/M2 channels were first inhibited by various concentrations of amantadine ( $1$ – $100\ \mu\text{M}$ ) for 60 s; then, BL-1743 ( $100\ \mu\text{M}$ ) was substituted for amantadine in the activating solution for 90 s (Figure 6). The lower the amantadine concentrations, the greater the effect of BL-1743 inhibition as evidenced by more current recovered after the 5 min

long washout (Figure 6A,B). When amantadine was applied at a saturating concentration ( $100\ \mu\text{M}$ ), substitution with BL-1743 did not add to the existing inhibition by amantadine (Figure 6D).

Taken together, these results suggest competition between BL-1743 and amantadine for inhibition of the A/M2 channel and support the conclusion that amantadine inhibits A/M2 channel activity by binding inside the channel pore. The results of this competition study also are in a good agreement with the amantadine inhibition kinetic rates reported by Wang et al. (25).

The reaction rate constants for the spiran amine compounds were not precisely determined; however, as shown in Figure 4C, the washout rate for the spiran amine **8** was not significantly different from that of amantadine, suggesting it should behave like amantadine.

**Voltage Dependence of Inhibition of A/M2 Channel Activity by Amantadine, BL-1743, and Spiran Amine.** Since spiran amine **8** is a positively charged molecule in aqueous solution over the pH range used in this study, its inhibitory effect on A/M2 channels may depend on membrane voltage. To address this possibility, we tested the voltage dependence of A/M2 channel inhibition by spiran amine **8** and compared it to that of BL-1743, spiro piperidine **20**, and amantadine. Previous studies have shown that the inhibition of A/M2 channel activity by BL-1743 does not depend on voltage (9), while the voltage dependence of amantadine inhibition has not been addressed directly. We observed that inward and outward A/M2 channel currents measured in the presence of each of the tested



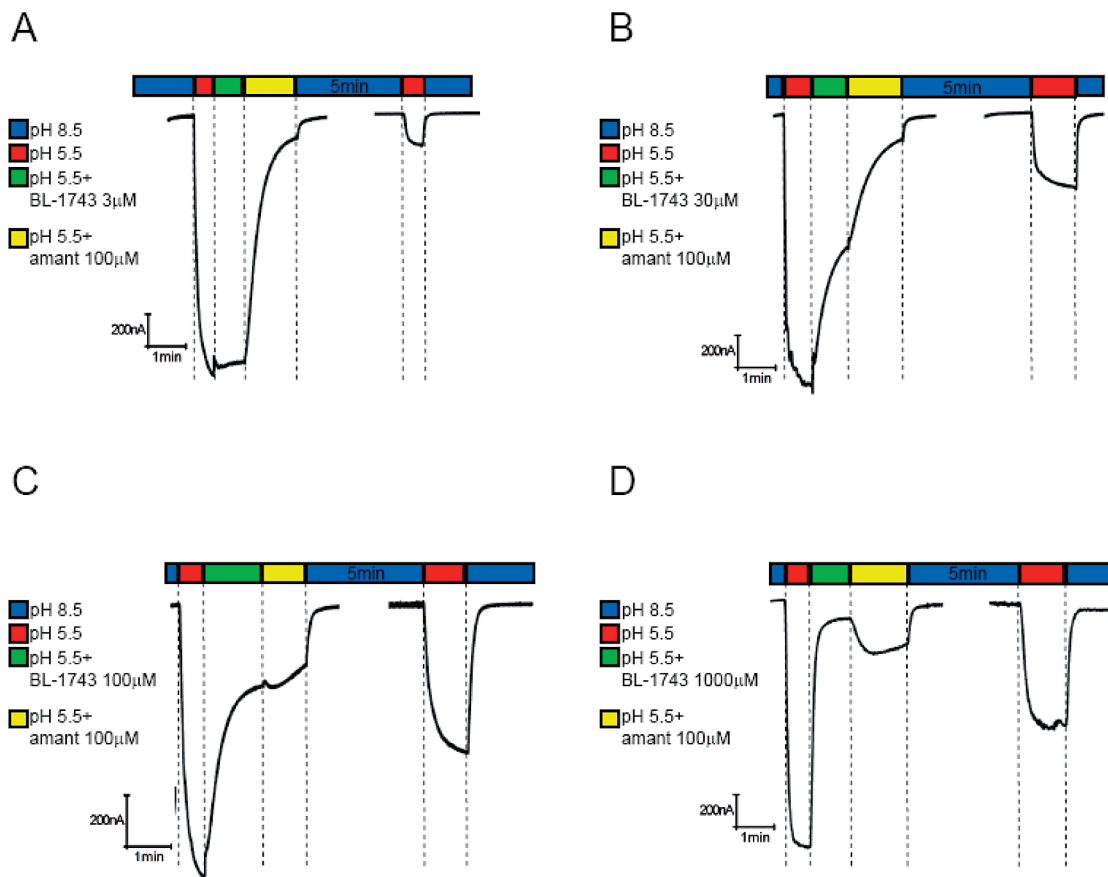


FIGURE 5: Inhibition of A/M2 channel activity by consecutive application of BL-1743 and amantadine. (A–D) Representative traces of the A/M2 channel activity modulated by consecutive application of BL-1743 and amantadine. A/M2 channel activity was induced by the application of the activating solution (pH 5.5, red horizontal bar above the trace). The currents were first inhibited by the application of the activating solution (pH 5.5) containing various concentrations of BL-1743 (3–1000  $\mu$ M, green horizontal bar) for 60 s. After maximal inhibition of the channel activity was achieved, amantadine (100  $\mu$ M) was substituted for BL-1743 (3–1000  $\mu$ M) in the activating solution for 90 s (yellow horizontal bar). The inhibitors were washed out for 5 min by the nonactivating solution (pH 8.5, second blue horizontal bar), and the pH-induced activity of A/M2 channels was measured again (second red horizontal bar). Note the biphasic current upon application of amantadine during washout of a saturating concentration of BL-1743 (during the yellow bar in panel D).

compounds were equally inhibited in the voltage range from –40 to 40 mV (Figure 7). These findings indicate that inhibition by none of the tested compounds is voltage-dependent.

## DISCUSSION

As amantadine-resistant influenza A strains become prevalent, the need for novel small molecule inhibitors grows. Our previous SAR of the BL-1743 series of compounds revealed one tight binding inhibitor, spiro piperidine **20** with an  $IC_{50}$  of 0.9  $\mu$ M, which has been shown to perturb a larger region in the pore-lining area of wt A/M2 than amantadine (10). In our study, an additional set of compounds was made by converting the spiro piperidine scaffold to spiran amine, which still retains the conformation of spirocycles for tight binding but has a slightly more extended structure. Compound **8** from this series shows promising inhibitory activity against two of the naturally occurring A/M2 point mutants: A/M2-L26F and A/M2-V27A (Figure 2). L26 and V27 are the residues closest to the channel exterior (Figure 8) to have been associated with amantadine resistance in naturally occurring mutants of A/M2 (12, 16, 34). It is interesting to note that, although L26F and V27A were inhibited by **8**, none of the amantadine-insensitive mutants located deeper in the pore was sensitive to spirane amine **8** (Table 2). However, of these, only S31N poses a significant clinical threat.

Panels A and B of Figure 8 illustrate the position of L26 and V27 in the crystal structure of the transmembrane domain of A/M2 complexed with amantadine at low pH, while panel C shows a model of the complex at high pH in phospholipid bilayers obtained by solid-state NMR (12). Although there are significant differences between the details of these and other experimental models (35, 36), V27 projects directly toward the pore while L26 is critical for packing at the helix–helix interface. Thus, changes to residues at these positions are likely to cause changes to the N-terminal region of the channel lumen, precisely at a location where amantadine has been found to bind. We are currently conducting crystallographic and molecular dynamics analyses of these mutants to determine their effect on the channel structure, and also to define the mechanism by which compound **8** is able to inhibit these otherwise drug-resistant variants. However, it is inviting to speculate that the decrease in hydrophobicity and steric bulk associated with the V27A mutation might increase the polarity and pore radius near the N-terminal region of the binding site. In this scenario, the extended length of compound **8** would provide increased steric and physicochemical complementarity to the variants, particularly its amine group projected outward toward the exterior of the virus.

It was previously shown that BL-1743 inhibits A/M2 channel activity by binding inside the channel pore with the  $\kappa_{on}$  kinetic similar to that of amantadine, but with a nearly 10-fold faster



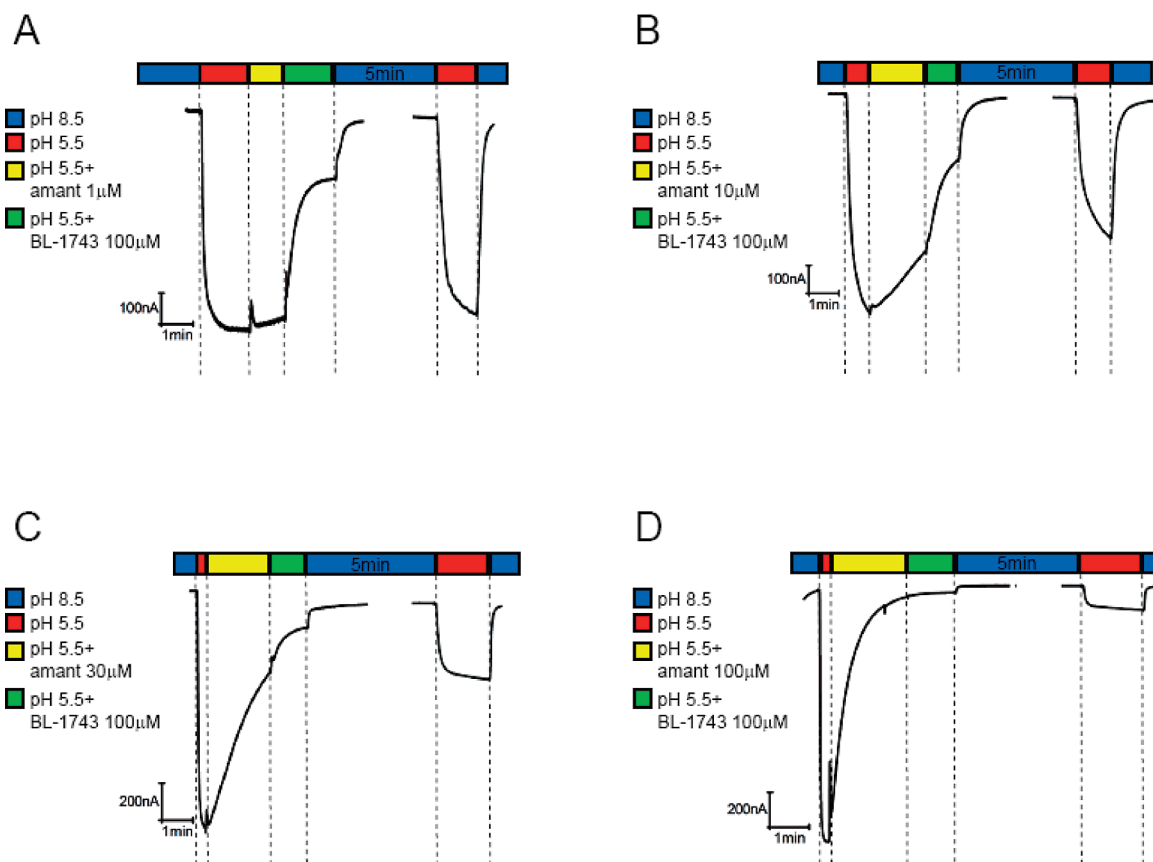


FIGURE 6: Inhibition of A/M2 channel activity by consecutive application of amantadine and BL-1743. (A–D) Representative traces of the A/M2 channel activity modulated by consecutive application of amantadine and BL-1743. A/M2 channel activity was induced by the application of the activating solution (pH 5.5, red horizontal bars above the traces). The currents were first inhibited by the application of the activating solution (pH 5.5) containing various concentrations of amantadine (1–100  $\mu$ M, yellow horizontal bar) for 60 s. After the maximal inhibition of the channel activity was achieved, BL-1743 (100  $\mu$ M) was substituted for amantadine (1–100  $\mu$ M) in the activation for 90 s (green horizontal bar). The inhibitors were washed out for 5 min by the nonactivating solution (pH 8.5, second blue horizontal bar), and the pH-induced activity of A/M2 channels was measured again (second red horizontal bar). Note that in no instance was a biphasic current observed during application of BL-1743 as amantadine was washed out (yellow bars).

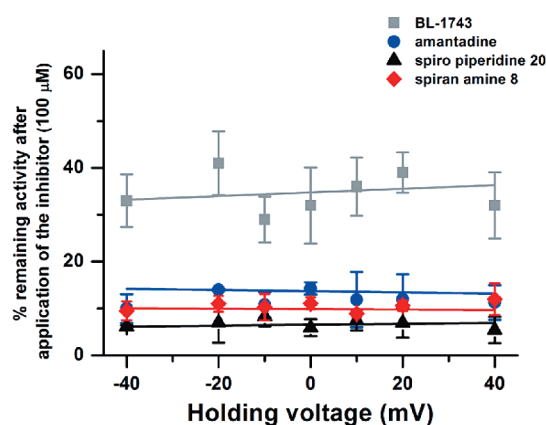


FIGURE 7: Voltage dependence of A/M2 inhibition by amantadine, BL-1743, spiro amine 8, and spiro piperidine 20. Inhibition of A/M2 channel activity by amantadine, BL-1743, spiro amine 8, and spiro piperidine 20 was assayed at various holding voltages (from –40 to 40 mV). The mean ( $\pm$ standard deviation) channel activity remaining after the maximal inhibition by each of the inhibitors (100  $\mu$ M) was achieved was plotted as a function of the holding voltage. The experimental data are the average of three independent experiments. Each point is a mean ( $\pm$ standard deviation) of 6–10 oocytes.

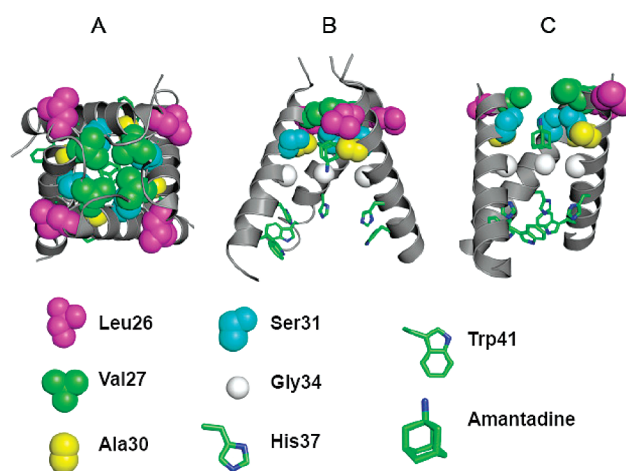


FIGURE 8: Structure of amantadine complexes with the transmembrane domain of A/M2 protein. Panels A and B illustrate the crystal structure of the channel (Protein Data Bank entry 3K9J) viewed from the outside of the virus (A) and in a side-on view with the on helix removed for the sake of clarity (B). Panel C shows a lower-resolution model (Protein Data Bank entry 2KAD) obtained from an analysis of solid-state NMR angular and distance restraints. The identities of critical residues are shown below, showing the C- $\alpha$  and side chain atoms.

$\kappa_{\text{off}}$  kinetic (9, 25). By employing the differences in the kinetic properties of amantadine and BL-1743 inhibition, we tested whether these two compounds compete for the same binding

site. Figure 5D shows that when A/M2 channels are occupied with BL-1743, after amantadine substitution for BL-1743 in the

recording solution, no additional inhibition by amantadine occurs, and slow reinitiation of amantadine binding starts only as the unbinding of rapidly reversible BL-1743 occurs. These findings are consistent with bound BL-1743 molecules preventing the channel from binding amantadine. Since BL-1743 binds in the pore, this result indicates that amantadine also inhibits A/M2 channel activity by binding in the channel pore.

As amantadine, BL-1743, and spirane amine **8** are all easily protonated in the pH range used in this study, and it is often observed that the efficacy of a positively charged channel inhibitor increases as membrane voltage is made more negative, we tested the voltage dependence of these compounds and of spiro piperidine **20** in the range of  $-40$  to  $40$  mV. Earlier electrophysiological characterizations of A/M2 inhibition by BL-1743 revealed that the inhibition was not voltage-dependent (9). Our study confirms the voltage independence of BL-1743, amantadine, spiro piperidine **20**, and spirane amine **8** (Figure 7). This finding is consistent with the location of the binding site occurring on the N-terminal half of the pore in a location exterior (N-terminal in peptide sequence) to the Trp/His gate, over which the transmembrane voltage drop is expected to occur. This binding mode is also consistent with the site inferred from solid-state NMR measurements of the perturbation to channel resonances associated with binding of spiro piperidine **20** (10). Furthermore, the existence of mutants conferring BL-1743 resistance (9, 24) suggests that the drug binding site is located on the extracellular-facing portion of the pore, N-terminal of H37. The lack of voltage dependence of amantadine inhibition and failure for intracellularly injected amantadine to inhibit (37) are also consistent with this binding location and argue against a proposed mechanism of amantadine binding to the outer intracellular-facing side of the pore of the protein (21, 22).

Together, these data argue for the previously proposed mode of binding to the pore of the channel (14–17). However, assuming the voltage drop occurs at the His/Trp gate, these data do not differentiate models in which the positively charged ammonium (or guanidinium group of BL-1743) of the drugs is directed toward the viral exterior or downward toward the H37 residues. It also should be kept in mind that the lack of a voltage dependence might occur if the binding of the positively charged inhibitor occurs in an exchange in which one proton is released to the outside of the cell when one inhibitor molecule enters the pore without changing the total charge inside the pore. While this is a formal possibility that is consistent with the fact that the binding of drug occurs with concomitant loss of one or more protons from the H37 residues (38), it seems unlikely that the proton release would obligatorily occur to the exterior, rather than the interior, which is the natural direction of proton flow.

In summary, these results demonstrate the feasibility of designing antiviral drugs effective against amantadine-resistant escape mutants of influenza A virus. Relatively modest modifications to BL-1743 have now resulted in a potent inhibitor of two naturally occurring A/M2 amantadine-insensitive mutants: A/M2-L26F and A/M2-V27A. Moreover, the electrophysiological experiments lend support to the existence of the binding site in the outer portion of the channel pore (12, 15, 16, 23, 34). Thus, three-dimensional models in which the drug is bound in the N-terminal regions of the pore should provide useful starting points for the design of even more tight-binding and broad-spectrum agents.

## SUPPORTING INFORMATION AVAILABLE

Chemical synthesis of the compounds and the CD titration assay. This material is available free of charge via the Internet at <http://pubs.acs.org>.

## REFERENCES

- Cox, N. J., and Subbarao, K. (1999) Influenza. *Lancet* 354, 1277–1282.
- Lagoja, I. M., and De Clercq, E. (2008) Anti-influenza virus agents: Synthesis and mode of action. *Med. Res. Rev.* 28, 1–38.
- Deyde, V. M., Xu, X., Bright, R. A., Shaw, M., Smith, C. B., Zhang, Y., Shu, Y., Gubareva, L. V., Cox, N. J., and Klimov, A. I. (2007) Surveillance of resistance to adamantanes among influenza A(H3N2) and A(H1N1) viruses isolated worldwide. *J. Infect. Dis.* 196, 249–257.
- Hay, A. J., Wolstenholme, A. J., Skehel, J. J., and Smith, M. H. (1985) The molecular basis of the specific anti-influenza action of amantadine. *EMBO J.* 4, 3021–3024.
- Garten, R. J., Davis, C. T., Russell, C. A., Shu, B., Lindstrom, S., Balish, A., Sessions, W. M., Xu, X., Skepner, E., Deyde, V., Okomo-Adhiambo, M., Gubareva, L., Barnes, J., Smith, C. B., Emery, S. L., Hillman, M. J., Rivaller, P., Smagala, J., de Graaf, M., Burke, D. F., Fouchier, R. A., Pappas, C., Alpuche-Aranda, C. M., Lopez-Gatell, H., Olivera, H., Lopez, I., Myers, C. A., Faix, D., Blair, P. J., Yu, C., Keene, K. M., Dotson, P. D., Boxrud, D., Sambol, A. R., Abid, S. H., St George, K., Bannerman, T., Moore, A. L., Stringer, D. J., Blevins, P., Demmler-Harrison, G. J., Ginsberg, M., Kriner, P., Waterman, S., Smole, S., Guevara, H. F., Belongia, E. A., Clark, P. A., Beatrice, S. T., Donis, R., Katz, J., Finelli, L., Bridges, C. B., Shaw, M., Jernigan, D. B., Uyeki, T. M., Smith, D. J., Klimov, A. I., and Cox, N. J. (2009) Antigenic and Genetic Characteristics of Swine-Origin 2009 A(H1N1) Influenza Viruses Circulating in Humans. *Science* 325, 197–201.
- Pinto, L. H., and Lamb, R. A. (2007) Controlling influenza virus replication by inhibiting its proton channel. *Mol. Biosyst.* 3, 18–23.
- Pinto, L. H., and Lamb, R. A. (2006) The M2 proton channels of influenza A and B viruses. *J. Biol. Chem.* 281, 8997–9000.
- Hu, J., Fu, R., Nishimura, K., Zhang, L., Zhou, H. X., Busath, D. D., Vijayvergiya, V., and Cross, T. A. (2006) Histidines, heart of the hydrogen ion channel from influenza A virus: Toward an understanding of conductance and proton selectivity. *Proc. Natl. Acad. Sci. U.S.A.* 103, 6865–6870.
- Tu, Q., Pinto, L. H., Luo, G., Shaughnessy, M. A., Mullaney, D., Kurtz, S., Krystal, M., and Lamb, R. A. (1996) Characterization of inhibition of M2 ion channel activity by BL-1743, an inhibitor of influenza A virus. *J. Virol.* 70, 4246–4252.
- Wang, J., Cady, S. D., Balannik, V., Pinto, L. H., DeGrado, W. F., and Hong, M. (2009) Discovery of spiro-piperidine inhibitors and their modulation of the dynamics of the M2 proton channel from influenza A virus. *J. Am. Chem. Soc.* 131, 8066–8076.
- Bright, R. A., Shay, D. K., Shu, B., Cox, N. J., and Klimov, A. I. (2006) Adamantane resistance among influenza A viruses isolated early during the 2005–2006 influenza season in the United States. *JAMA, J. Am. Med. Assoc.* 295, 891–894.
- Cady, S. D., Mishanina, T. V., and Hong, M. (2009) Structure of amantadine-bound M2 transmembrane peptide of influenza A in lipid bilayers from magic-angle-spinning solid-state NMR: The role of Ser31 in amantadine binding. *J. Mol. Biol.* 385, 1127–1141.
- Furuse, Y., Suzuki, A., and Oshitani, H. (2009) Large-Scale Sequence Analysis of M Gene of Influenza A Viruses from Different Species: Mechanisms for Emergence and Spread of Amantadine Resistance. *Antimicrob. Agents Chemother.* 53, 4457–4463.
- Duff, K. C., Gilchrist, P. J., Saxena, A. M., and Bradshaw, J. P. (1994) Neutron diffraction reveals the site of amantadine blockade in the influenza A M2 ion channel. *Virology* 202, 287–293.
- Stouffer, A. L., Acharya, R., Salom, D., Levine, A. S., Di Costanzo, L., Soto, C. S., Tereshko, V., Nanda, V., Stayrook, S., and DeGrado, W. F. (2008) Structural basis for the function and inhibition of an influenza virus proton channel. *Nature* 451, 596–599.
- Yi, M., Cross, T. A., and Zhou, H. X. (2008) A secondary gate as a mechanism for inhibition of the M2 proton channel by amantadine. *J. Phys. Chem. B* 112, 7977–7979.
- Chen, H., Wu, Y., and Voth, G. A. (2007) Proton transport behavior through the influenza A M2 channel: Insights from molecular simulation. *Biophys. J.* 93, 3470–3479.
- Khurana, E., Dal Peraro, M., DeVane, R., Vempalala, S., DeGrado, W. F., and Klein, M. L. (2009) Molecular dynamics calculations suggest a conduction mechanism for the M2 proton channel from influenza A virus. *Proc. Natl. Acad. Sci. U.S.A.* 106, 1069–1074.

19. Bright, R. A., Medina, M. J., Xu, X., Perez-Oronoz, G., Wallis, T. R., Davis, X. M., Povinelli, L., Cox, N. J., and Klimov, A. I. (2005) Incidence of adamantane resistance among influenza A (H3N2) viruses isolated worldwide from 1994 to 2005: A cause for concern. *Lancet* 366, 1175–1181.
20. Saito, R., Sakai, T., Sato, I., Sano, Y., Oshitani, H., Sato, M., and Suzuki, H. (2003) Frequency of amantadine-resistant influenza A viruses during two seasons featuring cocirculation of H1N1 and H3N2. *J. Clin. Microbiol.* 41, 2164–2165.
21. Schnell, J. R., and Chou, J. J. (2008) Structure and mechanism of the M2 proton channel of influenza A virus. *Nature* 451, 591–595.
22. Pielak, R. M., Schnell, J. R., and Chou, J. J. (2009) Mechanism of drug inhibition and drug resistance of influenza A M2 channel. *Proc. Natl. Acad. Sci. U.S.A.* 106, 7379–7384.
23. Jing, X., Ma, C., Ohigashi, Y., Oliveira, F. A., Jardetzky, T. S., Pinto, L. H., and Lamb, R. A. (2008) Functional studies indicate amantadine binds to the pore of the influenza A virus M2 proton-selective ion channel. *Proc. Natl. Acad. Sci. U.S.A.* 105, 10967–10972.
24. Gandhi, C. S., Shuck, K., Lear, J. D., Dieckmann, G. R., DeGrado, W. F., Lamb, R. A., and Pinto, L. H. (1999) Cu(II) inhibition of the proton translocation machinery of the influenza A virus M2 protein. *J. Biol. Chem.* 274, 5474–5482.
25. Wang, C., Takeuchi, K., Pinto, L. H., and Lamb, R. A. (1993) Ion channel activity of influenza A virus M2 protein: Characterization of the amantadine block. *J. Virol.* 67, 5585–5594.
26. Flaugh, M. E., Crowell, T. A., and Farlow, D. S. (1980) Acid-catalyzed annelation of  $\alpha$ -alkylaldehydes and  $\alpha,\beta$ -unsaturated ketones. A one-pot synthesis of 4,4-dimethyl-2-cyclohexen-1-one. *J. Org. Chem.* 45, 5399–5400.
27. Chan, Y., and Epstein, W. W. (1988) 4,4-Dimethyl-2-cyclohexen-1-one. *Org. Synth.* 50, 496–498.
28. Turner, R. M., Lindell, S. D., and Lay, S. V. (1991) A Facile Route to Imidazol-4-yl Anions and Their Reaction with Carbonyl Compounds. *J. Org. Chem.* 56, 5739–5740.
29. Balannik, V., Lamb, R. A., and Pinto, L. H. (2008) The oligomeric state of the active BM2 ion channel protein of influenza B virus. *J. Biol. Chem.* 283, 4895–4904.
30. Shimbo, K., Brassard, D. L., Lamb, R. A., and Pinto, L. H. (1996) Ion selectivity and activation of the M2 ion channel of influenza virus. *Biophys. J.* 70, 1335–1346.
31. Takeda, M., Pekosz, A., Shuck, K., Pinto, L. H., and Lamb, R. A. (2002) Influenza A virus M2 ion channel activity is essential for efficient replication in tissue culture. *J. Virol.* 76, 1391–1399.
32. Li, D., Saito, R., Suzuki, Y., Sato, I., Zaraket, H., Dapat, C., Caperig-Dapat, I. M., and Suzuki, H. (2009) In vivo and in vitro alterations in influenza A/H3N2 virus M2 and hemagglutinin genes: Effect of passage in MDCK-SIAT1 cells and conventional MDCK cells. *J. Clin. Microbiol.* 47, 466–468.
33. Stouffer, A. L., Nanda, V., Lear, J. D., and DeGrado, W. F. (2005) Sequence determinants of a transmembrane proton channel: An inverse relationship between stability and function. *J. Mol. Biol.* 347, 169–179.
34. Stouffer, A. L., Ma, C., Cristian, L., Ohigashi, Y., Lamb, R. A., Lear, J. D., Pinto, L. H., and DeGrado, W. F. (2008) The interplay of functional tuning, drug resistance, and thermodynamic stability in the evolution of the M2 proton channel from the influenza A virus. *Structure* 16, 1067–1076.
35. Pinto, L. H., Dieckmann, G. R., Gandhi, C. S., Papworth, C. G., Braman, J., Shaughnessy, M. A., Lear, J. D., Lamb, R. A., and DeGrado, W. F. (1997) A functionally defined model for the M2 proton channel of influenza A virus suggests a mechanism for its ion selectivity. *Proc. Natl. Acad. Sci. U.S.A.* 94, 11301–11306.
36. Hu, J., Asbury, T., Achuthan, S., Li, C., Bertram, R., Quine, J. R., Fu, R., and Cross, T. A. (2007) Backbone structure of the amantadine-blocked trans-membrane domain M2 proton channel from influenza A virus. *Biophys. J.* 92, 4335–4343.
37. Tang, Y., Venkataraman, P., Knopman, J., Lamb, R. A., and Pinto, L. H. (2005) The M2 proteins of Influenza A and B viruses are single-pass proton channels. In *Viral Membrane Proteins: Structure, Function and Drug Design* (Fischer, W. B., Ed.) pp 101–111, Kluwer Academic/Plenum Publishers, New York.
38. Li, C., Yi, M., Hu, J., Zhou, H. X., and Cross, T. A. (2008) Solid-state NMR and MD simulations of the antiviral drug amantadine solubilized in DMPC bilayers. *Biophys. J.* 94, 1295–1302.